ISBN: 978-3-95450-132-8 doi:10.18429/JACoW-IPAC2014-THPME017

ELECTROMECHANICAL ANALYSIS OF SCDTL STRUCTURES

M. Ciambrella, F. Cardelli, M. Migliorati, A. Mostacci, L. Palumbo,
Sapienza University of Rome, Italy
L. Ficcadenti, V. Pettinacci, INFN-Roma, Italy
L. Picardi, C. Ronsivalle, ENEA-Frascati, Italy

Abstract

The Side Coupled Drift Tube Linac (SCDTL) is a 3 GHz accelerating structure for proton therapy linac designed for TOP-IMPLART, an Intensity Modulated Proton Linear Accelerator for Radio-Therapy. The structure is made up of short DTL accelerating tanks for low current proton beams, coupled by side coupling cavities. The purpose of this paper is to report on the analysis of electromagnetic and the thermo-mechanical behavior for the SCDTL structure. The 3D electromagnetic analysis is used to derive the power dissipation on the structure; then one can infer the temperature distribution and deformation field in order to eventually evaluate their feedback on the electromagnetic properties of the structure as, for instance, the cavity resonant frequency shift. Such a "multi-physics" analysis has been performed for different supporting stem geometries in order to optimize the shunt impedance and the R/Q for SCDTL cavities.

ELECTROMECHANICAL ANALYSIS

The *power losses* (P_L) in the SCDTL [1] are due to the field interaction with its copper cavity surfaces. The detuning in the resonant regime, caused by the structural deformation due to the resulting heat loading, has to be monitored.

A two-ways coupling between the electromagnetic and the thermo-mechanical 3D analysis is necessary to quantify the "thermo-mechanical feedback" on the *resonant frequency* (f_0). Such electromechanical analysis is carried out with ANSYS codes, exploiting the coupling technology among multi-physics solvers of the ANSYS Workbench platform. Similar analysis has been reported in Ref. [2]. The ANSYS Workbench platform has made possible a different approach summarized in the following simulation flow:

1. ANSYS HFSS (Driven modal solver): electromagnetic simulation and calculation of f_0 for unperturbed condition and P_L;
2. ANSYS Mechanical (Steady-state thermal solver): geometry and P_L import, cooling system performances settings and calculation of the temperature distribution in working regime;
3. ANSYS Mechanical (Static structural solver): geometry and temperature distribution import, mechanical constraints settings and calculation of the deformation field (deformed geometry);
4. ANSYS HFSS (Driven modal solver): deformed geometry import and calculation of the new f_0 for the SCDTL working regime.

MODEL AND BOUNDARY CONDITIONS

The electromechanical analysis is performed for the smallest unit of the SCDTL structure, i.e. a single DTL accelerating tank without coupling cavities.

Model

Figure 1 shows the SCDTL model, which is directly drawn with the ANSYS HFSS 3D modeler. In addition to the copper structure and the accelerating cavity, there are the *cooling circuit* and the *waveguide-cavity coupler*. The cooling circuit consists of the eight cylindrical channels along the drift tube stems (*stem channels*), the two plena on both sides (*inlet* and *outlet plenum*) and the further cylindrical channel at the bottom (*bottom channel*). The design optimization of the coupler is not a significant problem in this case, as the best coupling affects the reflection coefficient module |S11| at the coupler port only, keeping unchanged the frequency for its minimum, i.e. the investigated f_0.

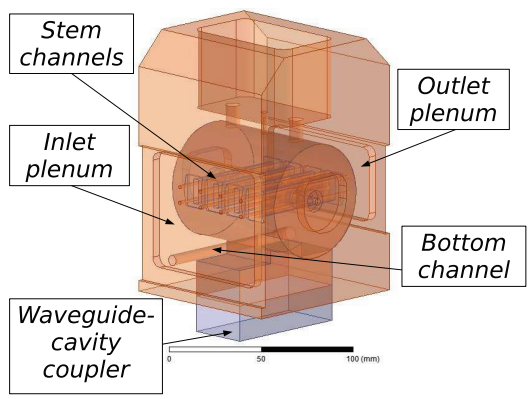

Figure 1: SCDTL model (only the copper surfaces of two plena on sides are visible).

Cooling System

Liquid water is the coolant. The water flow enters at the bottom channel, crosses it and goes to the inlet plenum: from here, it crosses the eight stem channels and then it is collected in the outlet plenum. The external cooling circuit, including the chiller, is not taken into account.

The boundary conditions for the thermal solver are a mean value of the convective heat transfer coefficient (h_{conv}) on the surfaces of each cooling system element, by considering the other surfaces as adiabatic.

The heat transfer mechanism across the stem and bottom channel surfaces is the *forced convection* for internal flows

ISBN: 978-3-95450-132-8 doi:10.18429/JACoW-IPAC2014-THPME017

[3]. The h_{conv} are calculated from the Nusselt number (Nu) as a function of the Prandtl (Pr) and Reynolds (Re) numbers:

$$Nu = \frac{h_{conv} D}{k}, \qquad Pr = \frac{\nu}{\alpha}, \qquad Re = \frac{Dv}{\nu},$$

where D is the channel diameter, v the fluid mean velocity, ν, α and k are water thermodynamic properties (respectively kinematic viscosity, thermal diffusivity and thermal conductivity).

The correlations $Nu = f(Pr, Re)$ to calculate h_{conv} depend on the water flow regime inside channels: the correlation for uniform heat flux is used for laminar flow (lam.), the Gnielinski's one for flow in transition (trans.) and the Dittus-Boelter's one for the turbulent flow (turb.) [3]. The water thermodynamic state is fixed by assuming its pressure and temperature constant and equal to, respectively, 0.1 MPa and to 40°C: thus ν, α, k are constant too. Also Pr is a thermodynamic property by definition, thus it is constant and equal to 4.33 according to [4].

Since D is fixed by SCDTL geometry, Re depends on v only. The electromechanical analysis are carried out for four assumed cooling modes (CMs), each one defined by a significant value for v in stem channels: the v in the bottom channel is consequently defined by the mass flow rate equation in the cooling circuit. Table 1 reports the h_{conv} assigned on the stem and bottom channel surfaces for each CM.

Table 1: Assumed Cooling Modes for Working Regimes

Cooling Modes		v [m/s]	Re	Flow regime	h_{conv} [W/m^{2}K]
#1	Stem	0.50	1520	lam.	1370
	Bottom	0.44	4052	trans.	2850
#2	Stem	1.00	3039	trans.	6110
	Bottom	0.89	8104	trans.	5720
#3	Stem	2.00	6234	trans.	13030
	Bottom	1.78	16208	turb.	10130
#4	Stem	3.50	10637	turb.	21700
	Bottom	3.11	28364	turb.	15970

The h_{conv} on the inlet and outlet plenum surfaces is fixed conservatively equal to 100 W/m^{2}K for all CMs.

Mechanical Constraints

The SCDTL external side, corresponding to the inlet plenum, is fastened on a support plane. The boundary condition for the structural solver is the assignment of the zero displacement on this surface.

RESULTS

Power Losses

Before export P_L from the electromagnetic to the thermal solver, we take into account that ANSYS HFSS computes the peak P_L, which have to be multiplied by the *duty cycle* (DC) of the power source to obtain the real heat loading for the structure. Moreover the coupler design is unoptimized thus the simulated electromagnetic field magnitude has a lower value than the expected one, i.e. the field when the coupler is optimized. The P_L depends on the square of the field, thus it has to be scale up to calculate the real detuning. Denoting with z the beam axis and with L the cavity axial length, the needed *scaling factor* (SF) is:

$$SF = \left(\frac{E^{OPT}}{E^{UNOPT}}\right)^2 = \left(\frac{\frac{1}{L}\int_0^L |E^{OPT}_{z,axis}|dz}{\frac{1}{L}\int_0^L |E^{UNOPT}_{z,axis}|dz}\right)^2.$$

By setting DC=0.0004 and, for beam dynamics reasons, E^{OPT}=15.62 MV/m, the P_L in the structure is 66.56 W.

Temperature Distributions

The temperature distribution is given by the equilibrium between the dissipated power on the cavity surfaces and the power removed by the water on the cooling system surfaces. The copper temperature is fixed at 22°C for the unperturbed condition. Table 2 reports the maximum and minimum temperature reached in the copper structure for each CM.

Table 2: Significant Temperatures for Each Cooling Mode

CM	T_{max} [°C]	T_{min} [°C]
#1	46.87	44.82
#2	43.17	41.59
#3	42.21	40.73
#4	41.84	40.42

Figure 2 shows the temperature distribution for CM#2. The higher temperatures are reached at the two extremal half drift tubes, because there is a significant power dissipation on their surfaces and the cooling elements are distant. The lower temperatures are reached in the structure portion in contact with the cooling surfaces, as expected.

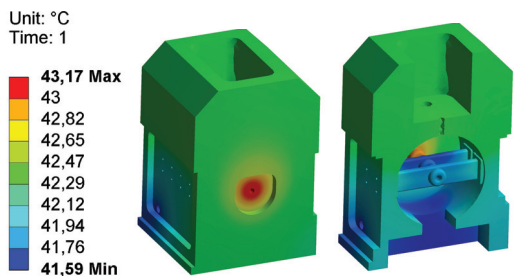

Figure 2: Temperature distribution for CM#2.

Deformation Fields

The temperature increase determines a deformation field in the structure, due to the thermal expansion coefficient of the copper and to the mechanical constraints. For all CMs the order of magnitude of the maximum deformation is few tens of microns, i.e. a value lower than the mechanical tolerance

ISBN: 978-3-95450-132-8 doi:10.18429/JACoW-IPAC2014-THPME017

and thus negligible from the structural point of view. Figure 3 shows the deformation distributions for CM#2.

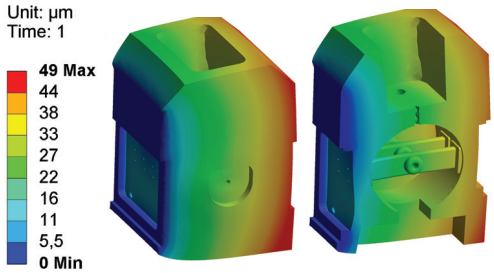

Figure 3: Deformation field for CM#2 (not in scale).

Detuning (Resonant Frequency Shifts)

Figure 4 shows the reflection coefficient |S11| against the frequency at the coupler port for unperturbed condition (blue line) and working regimes (purple line for CM#1, red line for CM#2, green line for CM#3, black line for CM#4).

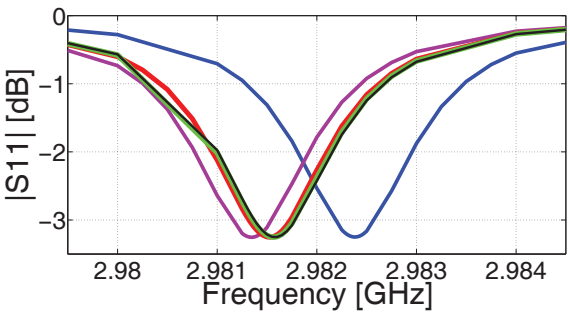

Figure 4: |S11| against frequency on the coupler port.

The f_0 for the unperturbed case is 2982.39 MHz. Table 3 reports the f_0, the *detuning* (Δf) and the *detuning per degree* ($\Delta f/\Delta T$) for different CMs. For each CM, the ΔT is the difference between the arithmetic mean temperature between the corresponding T_{max} and T_{min}, and 22°C , i.e. the temperature for the unperturbed condition.

Table 3: Detuning and f_0 for Working Regimes

CM	f [MHz]	Δf [MHz]	Δf/ΔT [kHz/°C]
#1	2981.35	-1.04	-43.62
#2	2981.53	-0.86	-42.20
#3	2981.57	-0.82	-42.12
#4	2981.60	-0.79	-41.30

DIFFERENT STEM GEOMETRIES

Figure 5 shows different stem geometries which have been investigated for SCDTL cavities. The OS cavity has the SCDTL design considered up to here. The DSS and SSS cavities have halved stems in order to reduce the dissipating copper surface: the halved stems are arranged alternatively on two opposite sides in the DSS cavity, and on the same side in the SSS one.

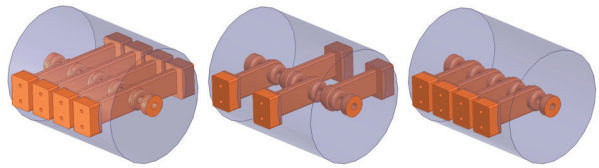

Figure 5: Alternative stems. FLTR: Original Stems (OS), Double Side Stems (DSS), Single Side Stems (SSS).

Table 4 reports the P_L and the R/Q for the cavity with different stem geometries: the P_L in the OS case is higher than 66.56 W, i.e. the losses previously calculated, because the coupler hole is neglected in this comparison and whole cavity is covered with copper. The halved stems determines a significant P_L reduction and a following increase of the cavity efficiency. Moreover the implementation of holes in the stem body has been investigated, but they introduce no significant enhancements for neither P_L and R/Q.

Table 4: P_L and R/Q for Different Stems

	OS	DSS	SSS
P_L [W]	72.97	53.70	57.98
R/Q [Ω]	831.07	873.29	867.90

CONCLUSIONS

The temperature distribution of the SCDTL structure is well related to the water temperature: thus a resonant frequency control can rely on the chiller action in the cooling circuit. Flow water velocity along stem channels higher than 2.0 m/s does not improve the cooling: even if we adopt a not reasonable value of 3.5 m/s, thus increasing the heat transfer very much, the temperature distribution is practically constant with respect to 2.0 m/s case. The electromechanical analysis carried out for all the assumed cooling modes shows the SCDTL structure detuning slightly is lower than -40 kHz per degree.

REFERENCES

[1] L. Picardi *et al.*, NIM A 425, 8-22 (1998)

[2] N. Hartman *et al.*, Proc. of PAC01, 912-914 (2001)

[3] F.P. Incropera *et al.*, *Fundamentals of Heat and Mass Transfer. Seventh Edition*, ISBN-13 9780470501979, Wiley (2011)

[4] W. Wagner *et al.*, JPCRD 31, 387-535 (2002)